

Magnetic fields in protoplanetary discs: from MHD simulations to ALMA observations

G. H.-M. Bertrang,^{1,2,3,4★} M. Flock⁵ and S. Wolf¹

¹Kiel University, Institute of Theoretical Physics and Astrophysics, Leibnizstr. 15, D-24118 Kiel, Germany

²Universidad de Chile, Departamento de Astronomía, Casilla 36-D, Santiago, Chile

³Universidad Diego Portales, Facultad de Ingeniería, Av. Ejército 441, Santiago, Chile

⁴Millennium Nucleus Protoplanetary Disks in ALMA Early Science, Universidad de Chile, Casilla 36-D, Santiago, Chile

⁵Jet Propulsion Laboratory, California Institute of Technology, Pasadena, California 91109, USA

Accepted 2016 September 7. Received 2016 September 7; in original form 2016 July 22

ABSTRACT

Magnetic fields significantly influence the evolution of protoplanetary discs and the formation of planets, following the predictions of numerous magnetohydrodynamic (MHD) simulations. However, these predictions are yet observationally unconstrained. To validate the predictions on the influence of magnetic fields on protoplanetary discs, we apply 3D radiative transfer simulations of the polarized emission of aligned aspherical dust grains that directly link 3D global non-ideal MHD simulations to Atacama Large Millimeter/submillimeter Array (ALMA) observations. Our simulations show that it is feasible to observe the predicted toroidal large-scale magnetic field structures, not only in the ideal observations but also with high-angular resolution ALMA observations. Our results show further that high-angular resolution observations by ALMA are able to identify vortices embedded in outer magnetized disc regions.

Key words: magnetic fields – polarization – radiation mechanisms: thermal – radiative transfer – protoplanetary discs.

1 INTRODUCTION

Magnetic fields play a crucial role in the formation and evolution of protoplanetary discs (Armitage 2011; Williams & Cieza 2011). Magnetic fields influence the transport of dust and gas (e.g. Ciesla 2007; Testi et al. 2014; Turner et al. 2014), the disc chemistry (e.g. Semenov & Wiebe 2011; Henning & Semenov 2013), and even the migration of planetesimals and planets within the disc (e.g. Dzyurkevich et al. 2010; Gressel, Nelson & Turner 2011; Uribe et al. 2011) through magnetohydrodynamic (MHD) turbulence. Moreover, MHD turbulence can provide the source of viscosity that drives the accretion (Lynden-Bell & Pringle 1974), and thus, the evolution of the disc (Shakura & Sunyaev 1973). One of the most promising mechanisms for driving turbulence, respectively, accretion is the magneto-rotational instability (Balbus & Hawley 1991; Balbus, Hawley & Stone 1996; Balbus & Hawley 1998). Turbulence generated by pure hydrodynamical instabilities (Nelson, Gressel & Umurhan 2013; Klahr & Hubbard 2014; Lyra 2014) is not able to explain the observed accretion rates and disc lifetimes (Williams & Cieza 2011), despite such instabilities could become important in disc regions with low ionization (Turner et al. 2014). High enough ionization, and so magnetic activity, is expected in the inner disc regions due to thermal ionization (Umebayashi & Nakano 1988; Desch & Turner 2015) and also in the outer disc

regions due to interstellar radiation (e.g. Turner, Sano & Dzyurkevich 2007; Dzyurkevich et al. 2013; Cleeves et al. 2015; Flock et al. 2015). However, even the prediction of any magnetic field structure by observational constraints remains a difficult task. First polarimetric observations of protoplanetary discs performed with the Submillimeter Array (SMA), the Combined Array for Research in Millimeter-Wave Astronomy (CARMA), and the Very Large Array (VLA) indicate toroidal magnetic field structures (Stephens et al. 2013; Rao et al. 2014; Cox et al. 2015). Spatially resolved observations of polarized millimeter continuum emission of aligned aspherical dust grains are well suited to reveal the magnetic field structure in the protoplanetary disc (e.g. Weintraub, Goodman & Akeson 2000; Cho & Lazarian 2007). Though, polarimetry is strongly influenced by many factors (Bertrang & Wolf 2016). Taking the dust grain shape, dust grain alignment, magnetic field properties, the resolution of the observation, and the projection along the line of sight into account, we present a feasibility study on high-angular resolution polarimetric observations and their interpretation to validate MHD predictions on magnetic fields in protoplanetary discs.

2 METHODS AND MODEL

2.1 Framework

For this work, we combine state-of-the-art 3D non-ideal MHD simulations with a new Monte Carlo radiative transfer algorithm to

* E-mail: bertrang@das.uchile.cl

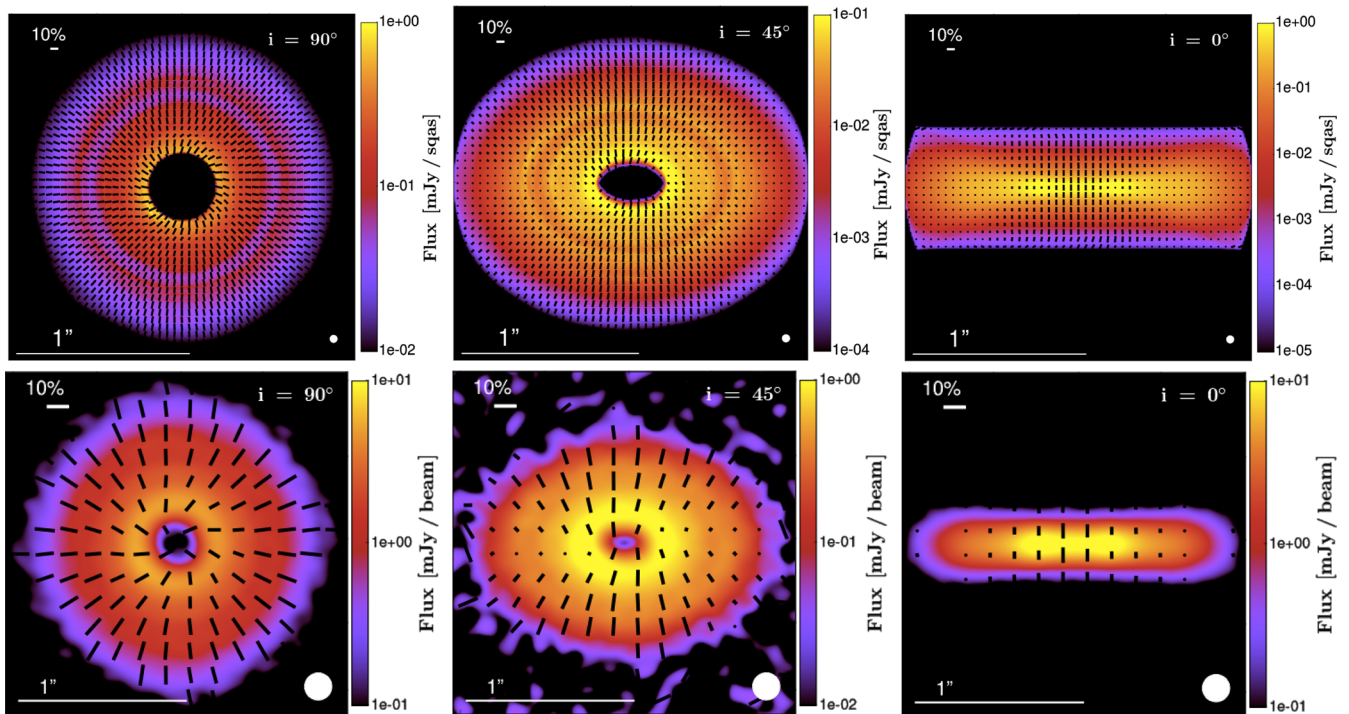


Figure 1. The ring state: self-consistent radiative transfer simulations of the polarized emission of aligned aspherical dust grains at 1.3 mm (top row), and simulated ALMA observations (bottom row; CASA v5.4.2, band 6, configuration C40-5, 1.5 h integration time; minimal displayed polarization degree is 1 per cent, i.e. the 3σ level of ALMA) at three different disc orientations (left: face-on, centre: 45° , right: edge-on). The colour map shows the total (unpolarized) intensity which is overlotted by polarization vectors. The vectors are plotted with the spatial resolution indicated by the beam size given as white ellipses. The toroidal magnetic field topology is traced by its characteristic polarization structure in all of the three orientations in the simulated ALMA observation.

calculate for the dust polarization emission. The resulting synthetic images are then post-processed with the Common Astronomy Software Applications (CASA) software package (v4.5.2) to obtain realistic Atacama Large Millimeter/submillimeter Array (ALMA) maps.

The 3D global non-ideal stratified MHD simulations were performed using the Fast Advection in Rotating Gaseous Objects (FARGO) MHD code PLUTO (Mignone et al. 2012; Flock et al. 2015).

The radiative transfer simulations are performed with an extended version of the code MC3D (Bertrang & Wolf 2016; Wolf, Henning & Stecklum 1999; Wolf 2003). We use the MHD models as input for the dust density distribution and magnetic field topology, and compute the temperature distribution, and anisotropy of the radiation field self-consistently. We assume aspherical dust grains with an axis ratio of 1: 1.3. We further assume here that the grains are perfectly aligned by the magnetic field. Based on these assumptions, we compute an upper limit for the polarized dust emission for aspherical grains.

Finally, to compare our MHD simulations with ALMA observations, we apply the CASA software package (v4.5.2). We simulate observations of 1.5h integration time at Band 6 (7.5GHz bandwidth) with the antennas configuration C40-5 and a spatial resolution of 0.16 arcsec. ALMA is able to detect the degree of polarization for resolved sources down to 0.3 per cent, along with an uncertainty of 6° in the polarization angle (ALMA Technical Handbook 2016).

2.2 Disc model

The disc model for the global 3D non-ideal MHD simulations follows an initial gas surface density of $\Sigma = 5.94 \text{g cm}^{-2} \left(\frac{100 \text{au}}{R}\right)$, with the cylindrical radius R . Temperature and density profiles are in

fully radiation hydrostatic equilibrium. The simulation domain in spherical coordinates spans from 20 to 100 au in radius, $\Delta\theta = 0.72$ rad in θ and full 2π in azimuth. We include an initial vertical magnetic field with a $1/R$ profile in radius. The initial resistivity profile is calculated using the dust chemistry method by Dzyurkevich et al. (2013), including HCO+ as dominant ion, electrons, and charged dust. For more details, we refer to model D2G_e-2 by Flock et al. (2015) (Section 2 and Fig. 1 therein).

For the radiative transfer simulations, we take two typical states of the global MHD simulations as input for the dust density structure and the magnetic field topology: the ring state, a state in which a axisymmetric gap and jump structure is present, and the vortex state, in which the ring shows a vortex and an enhanced density clump. Both states are emerging at the dead-zone edge, and for more details on the setup and models, we refer the reader to our previous works (Flock et al. 2015; Ruge et al. 2016). The model parameters are summarized in Table 1.

3 RESULTS

We aim at exploring the feasibility of high-angular resolution polarimetric observations and their interpretation to validate MHD predictions on magnetic fields in protoplanetary discs (for a discussion of the unpolarized dust emission, see Flock et al. 2015; Ruge et al. 2016). The questions arising from our MHD results are: can these magnetic field structures actually be traced? How can the differences between these models be detected to determine the physics taking place in a certain observational object? To answer these questions, we focus on simulated 1.3 mm maps of our models. We assume a distance to the disc of 100pc.

Table 1. Model parameters.

Parameter	Value
	Stellar properties
Distance (pc)	100
Effective temperature (K)	4000
Luminosity (L_{\odot})	0.95
Mass (M_{\odot})	0.5
	Disc parameters
Total mass (M_{\odot})	0.085
Gas-to-dust ratio	100
Disc inclination	$0^{\circ}, 45^{\circ}, 90^{\circ}$
	Dust parameters
Grain size distr. (μm)	$5e^{-2} - 1e^4$
Grain size distr. exponent	-3.5
Grain composition	Si (62.5 per cent), C (27.5 per cent)
Axis ratio	1.0:1.3
	Grid parameters
$N_r \times N_{\theta} \times N_{\phi}$	$256 \times 128 \times 512$
$\Delta r_{\text{au}} \times \Delta \theta_{\text{rad}} \times \Delta \phi_{\text{rad}}$	$20-100 \times 0.72 \times 2\pi$

In Figs 1 and 2, we present the post-processing radiative transfer simulations and simulated ALMA observations of the two typical states of the global MHD simulations at three different orientations of the disc. We find that the magnetic field topology as it is predicted by MHD simulations, can be validated by ALMA.

We find that the polarized signal can be traced across the extend of the disc, in both the ideal observation (the direct result of the radiative transfer simulation) as well as the simulated ALMA observation. The local degree of polarization lies between 1 per cent and 10 per cent (on a 3σ level) for the given model properties. While the degree of polarization in the ideal observation varies with the underlying density structure and disc inclination, it changes additionally with the noise level (i.e. the detection limit)

and spatial resolution (the lower the spatial resolution, the greater the impact of signal annihilation due to different polarization angles, e.g. an unresolved radial symmetric polarization pattern results in zero polarization) of the simulated interferometric measurement. This is caused by the sensitivity of the degree of polarization for projectional effects.

Further, we find that the polarized signal of a face-on disc shows a large-scale radial symmetric pattern, again in both the simulated ideal observation as well as the ALMA observation, for both models. Our MHD simulations show that the toroidal magnetic field topology continues within the density gaps (Flock et al. 2015), and accordingly, we find that the radial polarization pattern crosses these regions. Thus, the dust density gaps are traceable only by the unpolarized emission (and applying a higher spatial resolution, see Flock et al. 2015). However, we find clear deviations from the dominant toroidal structure inside the density enhancement region of the vortex which can be traced in the simulated face-on configuration (see Fig. 2, left).

At an inclination of 45° , we find a change in the radial polarization pattern towards a more homogenous, parallel structure. Towards the wings of the disc, the degree of polarization nulls. In the simulated ALMA observation, we find that the vortex can only be found in the total (unpolarized) intensity due to the density enhancement inside it. In comparison with the polarization signal in the ideal observation arising from the vortex at a face-on position, the polarization signal at an inclination of 45° appears to be altered by the vortex much less strongly. The spatial extent of the vortex in the polarization pattern appears to be reduced significantly (of the order of a factor of 2), and the change in the polarization angle and degree is accordingly smaller. These differences are not traced anymore in the simulated ALMA observation. Thus, the polarization patterns of the two typical states of the MHD simulations at this inclination are only distinguishable in the ideal observation, not in the simulated ALMA maps.

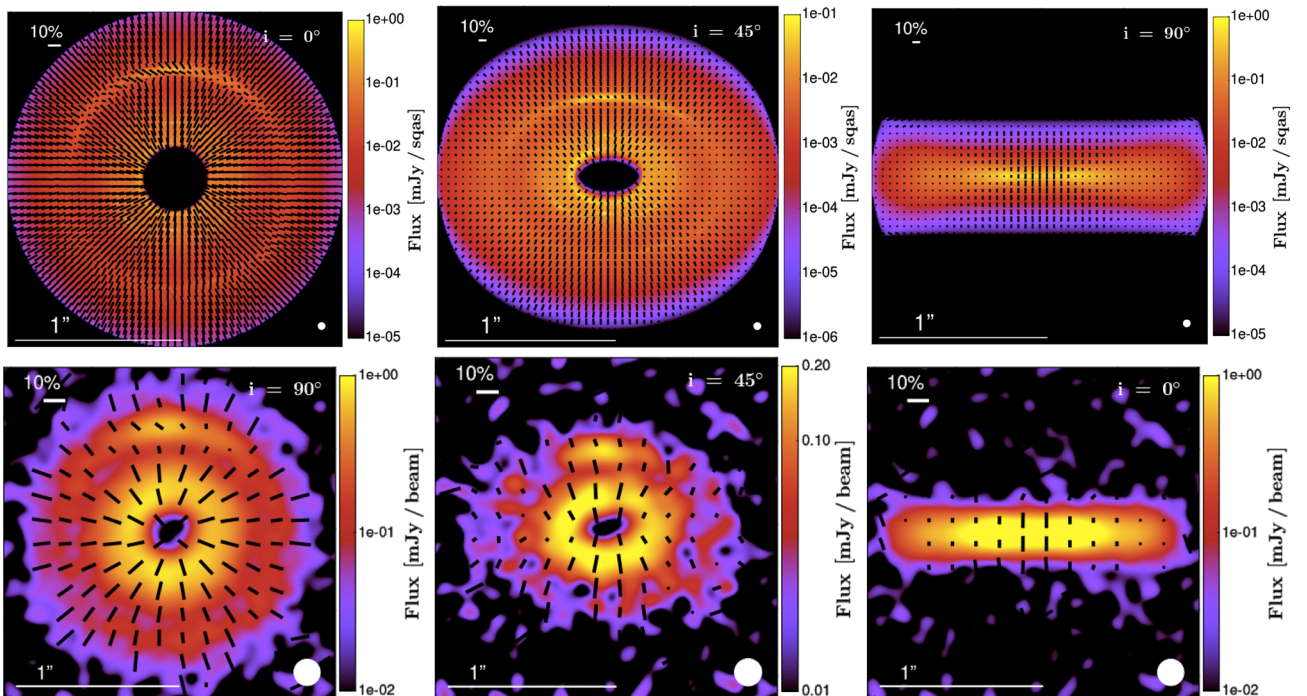


Figure 2. The vortex state: as in Fig. 1. The toroidal magnetic field topology is traced by its characteristic polarization structure in both orientations in the simulated ALMA observation, while the vortex is clearly detected in the simulated ALMA observation of a face-on disc.

Additionally, we find for an edge-on oriented disc that the resulting polarization pattern is homogenous and parallel in its orientation. The degree of polarization is maximal along the vertical centre axis of the disc and drops quickly towards the wings of the disc. This behaviour is typical for an underlying toroidal magnetic field structure and is also traced by the simulated ALMA observation. These findings as well as those of less inclined discs correspond to observations of the polarization pattern of younger (class I) protoplanetary discs that have been performed so far (Stephens et al. 2013, 2014), whilst the comparison to class II discs continues to wait for corresponding detections.

On the small spatial scales, we find that the polarized signal traces vortices in the magnetic field structure in both the degree of polarization and the orientation of the polarization pattern in the case of a face-on disc. Vertical components of the magnetic field as well as unordered field orientations in vortices, as resulting from our MHD simulations, act depolarizing due to projectional effects along the line-of-sight which emphasizes the importance of a full 3D disc model. Along the more ordered magnetic field lines found in large-scale vortices such as in Fig. 2, the orientation of the polarization pattern follows the vortex geometry. The vortex in the magnetic field structure alters the polarization pattern with respect to a purely radial structure locally by up to 90° in the polarization angle, and depolarizes the signal locally down to annihilation (Fig. 2). Our simulations show that these effects cannot only be seen in the ideal observations but also with high-angular resolution ALMA observations. The influence of vertical magnetic field components, however, is not traceable with the presented resolutions in the case of a more inclined disc.

4 SUMMARY AND CONCLUSION

We present a feasibility study on high-angular resolution polarimetric observations and their interpretation to validate MHD predictions on magnetic fields in protoplanetary discs. Based on the assumption of perfect grain alignment by the magnetic field, we compute an upper limit for the polarized dust emission for aspherical grains. This is consistent with previous work (Cho & Lazarian 2007) which was performed with less sophisticated models and lower spatial resolution. Our main results are as follows.

(i) In order to take radial and vertical magnetic field components correctly into account, a 3D disc model is vital for the simulation and interpretation of the polarized emission.

(ii) We find that the polarized signal which arises from aspherical grains aligned by the magnetic field does trace the magnetic field topology in both ideal observations and simulated ALMA observations. It has to be noted that the high-angular resolution of ALMA is critical for resolving the polarization pattern. Unresolved structure in the polarization pattern leads to annihilation of the signal.

(iii) Observations of the polarized emission of protoplanetary disc with ALMA are able to reveal the toroidal magnetic field structure. We have shown that it is even possible to observe small-scale deviations from the toroidal structure which could appear inside vortices located in the outer protoplanetary disc regions.

(iv) At an inclination of 45° , we find that small-scale structures in the magnetic field, such as a vortex, can only be observed with very high resolutions.

(v) For discs at lower inclination, we find polarization patterns corresponding to the observations of protoplanetary discs (class I) that have been performed so far. Detailed comparisons with observations of class II discs await future detections.

(vi) Gaps and jumps in the dust density distributions by magnetic activity as well as vertical magnetic field components in edge-on discs are still unresolved by the polarimetric observations.

ACKNOWLEDGEMENTS

GHMB acknowledges financial support by the Deutsche Forschungsgemeinschaft (DFG) under contract WO857/11-1 within the frame of the DFG Priority Program 1573: The Physics of the Interstellar Medium, as well as by the Millennium Science Initiative (Chilean Ministry of Economy), through grant Nucleus RC13007.

REFERENCES

- ALMA Technical Handbook 2016, ALMA Cycle 4 Technical Handbook. Available at: <https://almascience.nrao.edu/proposing/technical-handbook>
- Armitage P. J., 2011, *ARA&A*, 49, 195
- Balbus S. A., Hawley J. F., 1991, *ApJ*, 376, 214
- Balbus S. A., Hawley J. F., 1998, *Rev. Mod. Phys.*, 70, 1
- Balbus S. A., Hawley J. F., Stone J. M., 1996, *ApJ*, 467, 76
- Bertrang G. H.-M., Wolf S., 2016, *MNRAS*, in press
- Cho J., Lazarian A., 2007, *ApJ*, 669, 1085
- Ciesla F. J., 2007, *ApJ*, 654, L159
- Cleeves L. I., Bergin E. A., Qi C., Adams F. C., Öberg K. I., 2015, *ApJ*, 799, 204
- Cox E. G. et al., 2015, *ApJ*, 814, L28
- Desch S. J., Turner N. J., 2015, *ApJ*, 811, 156
- Dzyurkevich N., Flock M., Turner N. J., Klahr H., Henning T., 2010, *A&A*, 515, A70
- Dzyurkevich N., Turner N. J., Henning T., Kley W., 2013, *ApJ*, 765, 114
- Flock M., Ruge J. P., Dzyurkevich N., Henning T., Klahr H., Wolf S., 2015, *A&A*, 574, A68
- Gressel O., Nelson R. P., Turner N. J., 2011, *MNRAS*, 415, 3291
- Henning T., Semenov D., 2013, *Chem. Rev.*, 113, 9016
- Klahr H., Hubbard A., 2014, *ApJ*, 788, 21
- Lynden-Bell D., Pringle J. E., 1974, *MNRAS*, 168, 603
- Lyra W., 2014, *ApJ*, 789, 77
- Mignone A., Flock M., Stute M., Kolb S. M., Muscianisi G., 2012, *A&A*, 545, A152
- Nelson R. P., Gressel O., Umurhan O. M., 2013, *MNRAS*, 435, 2610
- Rao R., Girart J. M., Lai S.-P., Marrone D. P., 2014, *ApJ*, 780, L6
- Ruge J. P., Flock M., Wolf S., Dzyurkevich N., Fromang S., Henning T., Klahr H., Meheut H., 2016, *A&A*, 590, A17
- Semenov D., Wiebe D., 2011, *ApJS*, 196, 25
- Shakura N. I., Sunyaev R. A., 1973, *A&A*, 24, 337
- Stephens I. W. et al., 2013, *ApJ*, 769, L15
- Stephens I. W. et al., 2014, *Nature*, 514, 597
- Testi L. et al., 2014, in Beuther H., Klessen R. S., Dullemond C. P., Henning T., eds, *Protostars and Planets VI*. Univ. Arizona Press, Tucson, AZ, p. 339
- Turner N. J., Sano T., Dzyurkevich N., 2007, *ApJ*, 659, 729
- Turner N. J., Fromang S., Gammie C., Klahr H., Lesur G., Wardle M., Bai X.-N., 2014, in Beuther H., Klessen R. S., Dullemond C. P., Henning T., eds, *Protostars and Planets VI*. Univ. Arizona Press, Tucson, AZ, p. 411
- Umehayashi T., Nakano T., 1988, *Prog. Theor. Phys. Suppl.*, 96, 151
- Uribe A. L., Klahr H., Flock M., Henning T., 2011, *ApJ*, 736, 85
- Weintraub D. A., Goodman A. A., Akeson R. L., 2000, in Beuther H., Klessen R. S., Dullemond C. P., Henning T., eds, *Protostars and Planets IV*. Univ. Arizona Press, Tucson, AZ, p. 247
- Williams J. P., Cieza L. A., 2011, *ARA&A*, 49, 67
- Wolf S., 2003, *Comput. Phys. Commun.*, 150, 99
- Wolf S., Henning T., Stecklum B., 1999, *A&A*, 349, 839

This paper has been typeset from a $\text{\TeX}/\text{\LaTeX}$ file prepared by the author.